

MODELING AND DESIGN OF TWISTED TUBE HEAT EXCHANGERS

B. V. Dzyubenko

Moscow Aviation Institute
Moscow, Russia

L.-V. Ashmantas

Institute of Physico-Technical Problems
of Energetics of the Lithuanian Academy of Sciences
Vilnius, Lithuania

M. D. Segal

Kurchatov Atomic Energy Institute
Moscow, Russia

Edited by T. F. Irvine, Jr.

State University of New York, Stony Brook

Translated by

Irina Rybakova

BEGELL HOUSE INC. PUBLISHERS

New York

Modeling and Design of Twisted Tube Heat Exchangers

B.V. Dzyubenko, L.-V. Ashmantas, and M.D. Segal

Edited by T.F. Irvine, Jr.

Library of Congress Cataloging-in-Publication Data

Catalog record is available from the Library of Congress.

This book represents information obtained from authentic and highly regarded sources. Reprinted material is quoted with permission, and sources are indicated. A wide variety of references are listed. Every reasonable effort has been made to give reliable data and information, but the authors and the publisher cannot assume responsibility for the validity of all materials or for the consequences of their use.

All rights reserved. This book, or any parts thereof, may not be reproduced in any form without written consent from the publisher.

Direct all inquiries to Begell House, Inc., 79 Madison Avenue, New York, NY 10016.

© 2000 Begell House, Inc.

ISBN 1-56700-123-8

Printed in the United States of America 1 2 3 4 5 6 7 8 9 0

Preface

The book presents methods for numerically calculating heat and mass transfer in heat exchangers and facilities with channels formed by twisted tube bundles and porous heat transfer elements (PHE). Heat transfer in such devices is enhanced appreciably, which allows a reduction in their volume and amount of metal per structure [20, 23]. Moreover, a vigorous interchannel mixing of the heat-transfer fluid enables an improvement of output heat exchanger parameters and its operation reliability under conditions of high temperatures and heat flux densities. Therefore, heat exchangers with twisted tubes and PHE can be used successfully in aviation, power engineering, transport, chemical industry and other technological branches.

A one-dimensional description of processes in the heat-transfer fluid is normally used for the thermal hydraulic calculations of heat exchangers. In practice, however, a nonuniform heat supply (heat release) field is observed frequently in the cross section of a tube bundle which forms nonuniform temperature fields of the heat-transfer fluid in the intertubular space of a heat exchanger. Therefore, in the general case, consideration should be given to three-dimensional or axisymmetric problems with numerical calculations of steady and unsteady thermal hydraulic processes in complex-geometry channels in order to determine spatial temperature distributions in the heat-transfer fluid flows and the tube walls. Numerical modeling of these processes yields practical results without carrying out a great many expensive experiments.

For mathematical descriptions of steady and unsteady heat and mass transfer in twisted tube bundles and PHE, these studies employ a model of homogenized fluid flow which substitutes for the real flow in these devices [23]. In the case of an unsteady process, a model of homogenized fluid flow is defined by a system of equations which, alongside the equations of energy, momentum, continuity and state for the heat-transfer fluid, incorporates a heat conduction equation for a "solid phase", *viz.* twisted tubes or PHE. Here, a conjugate problem is solved with allowance for edge effects and the use of a heat transfer coefficient and an effective diffusion coefficient dependent on the boundary conditions.

Steady state problems of heat transfer in twisted tube bundles were solved numerically using various methods. In the case of an axisymmetric heat release nonuniformity in the bundle cross section, the most acceptable calculation method is that of matrix factorization extended by G. I. Marchuk to solving parabolic equations. The method was generalized to a homogenized fluid flow which is described by a system of parabolic equations with nonlinearities and coefficients dependent on the solution. Numerical analogs of the initial equations were written using an implicit finite-difference scheme. The steady state temperature fields for an axisymmetric heat release nonuniformity can be predicted also via a net-point method using an explicit scheme and a time-dependence technique based on replacing a steady state problem by a transient one and carrying the solution to a point when it no longer changes in time. The flow in a heat exchanger with PHE is described by a system of nonlinear differential equations of the elliptic type which are also solved by a time-dependence technique. Here, substituting a steady state problem by a transient one results in a system of parabolic equations solved by a method of alternating directions. Implicit schemes of the method allow wider variations of the relation of spatial-temporal steps, and convergence in the optimal case is attained with fewer iterations than using, for example, the method of successive over-relaxation generally applied to explicit schemes.

For numerical modeling of transient problems, a calculation technique was worked out based on separate solutions of the energy and heat conduction equations, and of the hydrodynamic equations correlated via the equation of state and iteration cycles. The energy and heat conduction equations were solved by the method of alternating directions both for axisymmetric and asymmetric heat release uniformities. Numerical analogs of the initial equations were defined here by an implicit scheme and solved by a factorization method delineated in the studies of A. A. Samarskiy, G. I. Marchuk, and N. N. Yanenko. The momentum and continuity equations were solved using McCormack's explicit two-step scheme of second-order accuracy. When written in a quasi-steady state approximation, the momentum and continuity equations were solved using a method of factorization with the aid of the Simuni substitution.

The theoretical aspects of numerical modeling of the thermal hydraulic processes in complex-geometry channels and the predictive techniques for these processes are followed by the presentation and description of block diagrams for the computation programs. Potentialities of the programs, and the questions as to the choice of the calculation net and integration steps, and the data input and output are also considered.

The monograph attaches a great deal of attention to experimentally substantiating the flow models and the systems of equations describing steady and unsteady thermal hydraulic processes. For this purpose, experimental and theoretical temperature fields of the heat-transfer fluid are compared. The systems of equations for steady and unsteady heat and mass transfer processes are closed

using empirical relations which determine the coefficients of heat transfer and hydraulic resistance and the effective diffusion coefficients in the function of governing dimensionless numbers. Here, along with linear relations in logarithmic coordinates, it is suggested to draw on second-order polynomials which in some cases better describe experimental data throughout the range of governing parameters and adequately reflect the physical nature of the heat and mass transfer processes. For processing experimental data and evaluating benefits of the proposed dimensionless relations, use is made of methods of statistical analysis of experimental data. Computerized automated systems of control of the experiment, and collection and processing of experimental data were employed in order to improve accuracy and dependability of the results obtained. Since the transient processes involving time variations in a heat load and a flow rate of the heat-transfer fluid are characterized by high rates of parametric variations and are in some cases governing, the unsteady heat and mass transfer was studied for different types of transient behavior.

The investigations allowed an ascertainment of a range of applications for the proposed dimensionless relations and a presentation of recommendations for practical calculations of heat and mass transfer under unsteady and steady conditions. The book analyzes and generalizes theoretical and experimental studies performed by the authors and other investigators.

Nomenclature

a	thermal diffusivity
c	specific heat
c_p	specific heat at constant pressure
d_{sh}	tube bundle diameter, $d_{sh} = 2r_{sh}$
d_e	equivalent diameter
D_t	effective diffusion coefficient
F	cross-sectional area of tubes in a bundle
F_b	area of the bundle flow section
F_x	projection of mass forces onto the axis x
G	mass flow rate of air
G_i	axial flow rate of the heat-transfer fluid in a cell
G_{ij}	lateral flow of the heat-transfer fluid from the cell i to the cell j per unit length of a channel
g	acceleration due to gravity
K	dimensionless effective diffusion coefficient
K_G	parameter characterizing the effect of a variation in the flow rate of the heat-transfer fluid
K_{sg}^*	parameter of thermaltransient behavior
K_α	ratio of the transient heat transfer coefficient to its quasi-steady value
L	spatial integral scale of turbulence
l	tube bundle length, mixing length
N	heat power
n	number of tubes in a bundle
q	heat flux density
q_w	heat flux density on the wall
q_v	density of internal heat sources
p	static pressure

p_t	total pressure
Δp	pressure drop
r	radial coordinate
r_{sh}	tube bundle radius
s	twist pitch of a tube profile
T	temperature
V	resultant velocity vector
u, v, w	components of the averaged velocity V in the orthogonal coordinate system
u', v', w'	fluctuating velocity components
u_r, u_t	tangential and radial velocity components in the cylindrical coordinate system
x	longitudinal coordinate
y	coordinate measured normally to the wall
α	heat transfer coefficient
δ	boundary layer thickness
ε	tube bundle porosity with respect to the heat-transfer fluid, $\varepsilon = F_b/F_\Sigma$
ε	relative transient diffusion coefficient
λ	thermal conductivity
μ	dynamic viscosity
ν	kinematic viscosity
ξ	hydraulic resistance
Π	channel perimeter
ρ	density
τ	time
φ	angular coordinate
χ	turbulence intensity
$ Fo$	Fourier number
$ Fr_M$	dimensionless number defining the flow swirling rate in a twisted tube bundle
$ Le$	Lewis number
$ Nu$	Nusselt number
$ Pr$	Prandtl number
$ Re$	Reynolds number

Subscripts

sh	heat exchanger shell
qs	quasi-steady

M	maximal, modified
n	transient
m	mean value, at mean temperature in the boundary layer
T	turbulent
s	"solid phase"
t	tube
ef	effective
b	mean mass quantity
d	determined from d_e
f	flow
r	directed along r
x	directed along the axis x
δ	obtained from the boundary layer thickness
τ	tangential
w	wall
1, 2	flow in twisted tubes and in an intertubular space

Contents

Preface	vi
Nomenclature	ix
1 Mathematical Description of Thermal Hydraulic Processes in Complex-Geometry Channels	1
1.1 Design Features of Heat Exchangers with Twisted Tubes and Porous Heat Transfer Elements	1
1.2 Initial System of Equations	10
1.3 Structural Features of Turbulent Flow in a Twisted Tube Bundle Allowing Simplification of its Mathematical Description	13
1.4 Systems of Equations for Thermal Hydraulic Processes in Twisted Tube Bundles. Calculated Flow Models	16
1.5 Specific Features of Numerical Modeling of Thermal Hydraulic Processes in Channels with PHE and Radial Flow	23
1.6 Dimensionless Relations for Transfer Coefficients Entering into the Motion and Energy Equations	26
2 Numerical Modeling of Steady Thermal Hydraulic Processes	34
2.1 Numerical Analogs of the Initial Systems of Equations for Flow in Twisted Tube Bundles	34
2.2 Writing Numerical Analogs of the Initial Equations at a Singular Point	38
2.3 Reducing Numerical Analogs of the Initial Equations to Vector-Matrix Form	40
2.4 Solving the Equations Using Matrix Factorization	43
2.5 Algorithm of Realizing the Predictive Technique	47
2.6 Structure of the RAPTIS Computation Program and its Potentialities	48
2.7 Description of the RAPTIS Program	50
2.8 Analysis of the Computation Error for the RAPTIS Program	53

2.9	Account of Edge Effects	55
2.10	Method of Solving the System of Equations for a Heat Exchanger with PHE. Finite-Difference Analogs of the Initial Equations	58
2.11	Solution Algorithm and Realization of Boundary Conditions	64
2.12	Examples of Numerical Calculations	66
3	Experimental Determination of Thermal Hydraulic Characteristics in Twisted Tube Bundles	70
3.1	Description of Experimental Setup, the Procedure of Processing Experimental Data for Heat Transfer and Hydraulic Resistance, and the Computation Programs	70
3.2	Results of Studying Heat Transfer. Empirical Relations for Calculating Heat Transfer	75
3.3	Results of Studying the Hydraulic Resistance. Empirical Relations for the Hydraulic Resistance Coefficient	83
4	Experimental Substantiation of Predictive Methods for Steady Heat Transfer Processes in Twisted Tube Bundles	89
4.1	Experimental and Data Processing Procedures. Statistical Analysis of the Results and Description of the Computation Program	89
4.2	Experimental Substantiation of the Physical Flow Model and Predictive Methods	99
4.3	Effect of the Shape of an Axisymmetric Heat Supply Nonuniformity on Transfer Coefficients	106
4.4	Effect of the Shape of an Asymmetric Heat Supply Nonuniformity on the Transfer Coefficient	110
4.5	Generalization of Experimental Data for Interchannel Mixing of the Heat-Transfer Fluid. Closing Similarity Equations	113
5	Numerical Modeling of Unsteady Thermal Hydraulic Processes in Twisted Tube Bundles	119
5.1	Selection of a Method for Solving the Initial System of Equations. Numerical Analogs	119
5.2	Solution Algorithm for a Transient Problem and Realization of Boundary Conditions	126
5.3	Quasi-Stationary Approximation and Methods of Solving the Problem	129
5.4	Structure and Capabilities of the DINA Program	130
5.5	Results for Unsteady Thermal Hydraulic Processes Computed by the DINA Program	133
5.6	Solution of the System of Three-Dimensional Transient Equations	134

6	Experimental Validation of Predictive Methods for Unsteady Heat and Mass Transfer in Twisted Tube Bundles	142
6.1	Distinctive Features of the Experimental Procedure for Studying Unsteady Heat and Mass Transfer. Description of an Experimental Setup	142
6.2	Effect of the Heat Load Variations on the Measured Temperature Fields of the Heat-Transfer Fluid. Experimental Validation of Predictive Methods	146
6.3	Heat and Mass Transfer with Variations in the Heat Load. Closing Empirical Relations	150
6.4	Heat and Mass Transfer with Variations in the Flow Rate of the Heat-Transfer Fluid. Empirical Relations for Closing the System of Equations	157
6.5	Specific Features of the Heat and Mass Transfer with Periodic Time Variations in the Flow Rate of the Heat-Transfer Fluid	170
6.6	Transient Temperature Fields of the Heat-Transfer Fluid for Asymmetric Heat Release Nonuniformity	174
7	Engineering Predictive Methods for Thermal Hydraulic Processes in Heat Exchangers	179
7.1	Calculation Steps for a Twisted-Tube Heat Exchanger	179
7.2	Calculation of a Twisted-Tube Heat Exchanged with Steady Operating Conditions. Scheme of the Computation Program	180
7.3	Taking Account of the Interchannel Mixing of the Heat-Transfer Fluid in the Intertubular Space of a Heat Exchanger. Scheme of the Computation Program and its Description	187
7.4	Computation of Transient Temperature Fields in Twisted Tube Bundles with a Nonuniform Heat Supply. Scheme of the Computation Program and its Description	195

1

Mathematical Description of Thermal Hydraulic Processes in Complex-Geometry Channels

1.1 Design Features of Heat Exchangers with Twisted Tubes and Porous Heat Transfer Elements

Among familiar techniques of heat and mass transfer enhancement, very promising is the method of flow swirling in complex-geometry channels formed by the bundles of twisted tubes of oval or three-blade profile [23] and a method relying on the use of porous heat transfer elements (PHE) [4, 20]. These methods are realized in heat exchangers of various structures with a great number of heat transfer elements (twisted tubes, granules, spheres, and others). Therefore, a model of homogenized fluid flow [23] appears to be the most promising for predicting temperature fields in such heat exchangers, although in some cases a channel-by-channel predictive method may be applied. As is well known, replacing the flow in a real twisted tube bundle (or in porous elements) by a homogenized fluid flow is an engineering technique. The use of this technique for predicting temperature and velocity fields in each specific case should be validated experimentally. Besides, the application of the model of homogenized fluid flow to each type of a heat exchanger has distinctions specified by the structural features of these devices.

Heat exchangers with a longitudinal flow past tubes may differ in the design of twisted tubes and their relative position. The most common structure of such a device is a heat exchanger with straight twisted tubes of oval profile[†], whose general view is presented in Fig. 1.1. The twisting of the oval profile of the tubes

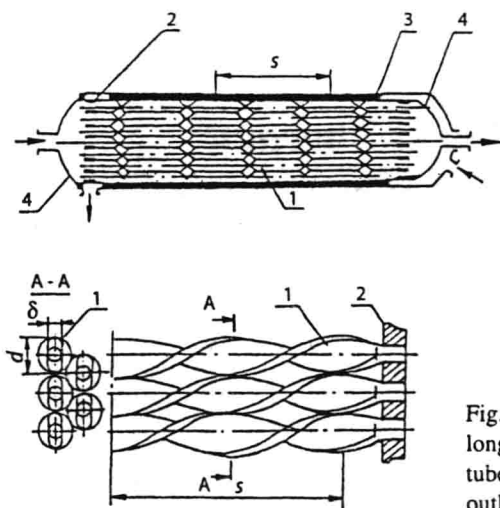


Fig. 1.1 General view of a heat exchanger with a longitudinal flow past twisted tubes: 1 – twisted tubes; 2 – tube boards; 3 – shell; and 4 – inlet and outlet tube stubs.

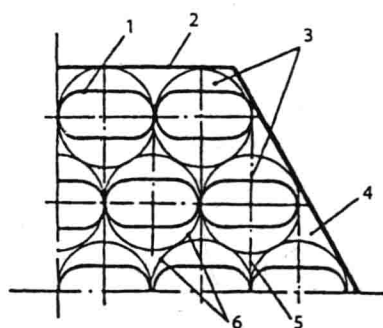


Fig. 1.2 Relative position of twisted tubes in a hexahedral shell when the structure is orderly: 1 – twisted tubes; 2 – shell; 3 – spiral channels; 4, 5 – straight-through channels for peripheral and central cells; and 6 – conventional boundaries of spiral and straight-through channels.

results in an intricate spatial flow of the heat-transfer fluid. A look at a fragment of the cross section of a twisted tube bundle (Fig. 1.2) reveals the characteristic flow regions in the channel for the heat-transfer fluid passage. A major part of the flow section is taken up by spiral channels, where the flow swirls past twisted tubes, which is longitudinal relative to their axes.

Examining a bundle with closely arranged tubes by transmitted light makes the straight-through channels (Fig. 1.2) visible. The cross-sectional area of a straight-through channel near the shell, on the heat exchange periphery, is noticeably larger than that of a straight-through channel in the central cells of the bundle. Although the straight-through channels only account for about 9–10% of the total area of the flow section, they have a certain impact on the flow structure in a

[†]Author's certificate 761820 USSR, B. V. Dzyubenko and Yu. V. Vilemas, Shell-and-Tube Heat Exchanger, B. I., 1980, No. 33, p. 194.

twisted tube bundle [3]. The twisted tube bundle is characterized also by a non-uniformity of the distribution of the bundle porosity with respect to the heat-transfer fluid depending on the heat exchanger radius or azimuth. Figure 1.3 illustrates the variation in the radial porosity of a 37-tube bundle with respect to the heat-transfer fluid, ϵ_r . Numerical modeling of thermal hydraulic processes should take account of these structural features of a twisted-tube heat exchanger.

Characteristic geometric parameters of twisted-tube heat exchangers are also affected by the number of tubes in a bundle. It is clear from Fig. 1.4 that, for bundles with few tubes ($n = 7$ or 19), the equivalent diameter of a bundle differs markedly from d_e for bundles with many tubes, and the perimeter of twisted tubes Π_t is much the smaller than the total bundle perimeter because of the contribution of the shell perimeter. The effect of the number of tubes in a bundle on its determining dimensions should be considered when experimentally obtaining, applying and closing the dimensionless equations for transfer coefficients in twisted tube bundles.

Design features of twisted tube bundles also specify the structure of a steady turbulent flow [3]. Let us examine the chief characteristics of a flow which illustrate the effect of flow swirling in central and peripheral bundle cells. The flow in central bundle cells is governed by the interaction of swirling flows in the spiral channels of neighboring tubes (Fig. 1.5). Here, tangential velocities in the flow core are distributed by the law of distribution of the tangential velocities induced by vortex filaments with opposite rotation directions. In this case, the radial

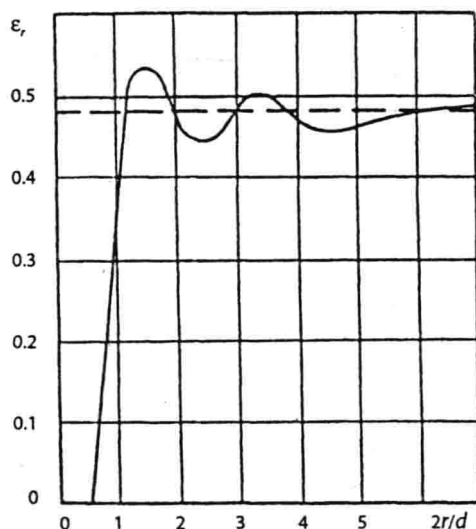


Fig. 1.3 Radial porosity of a twisted tube bundle with respect to the heat-transfer fluid vs radius: $\epsilon_r = f(2r/d)$, $--- \epsilon_{rm} = f(2r/d)$.

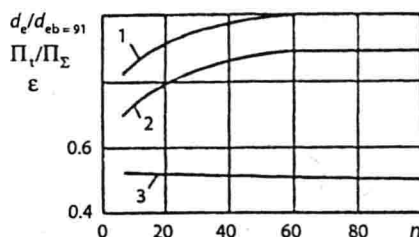


Fig. 1.4 Variation in the relative equivalent diameter (1) and perimeter (2) of tubes, and in the porosity (3) of a twisted tube bundle with the number of tubes in a bundle.

velocity u_r , in the cell center is directed from the tube wall to the flow core in the same way as on the windward side of the tube profile [23] but is appreciably smaller in magnitude. At the same time, u_r on the leeward side of the tube profile is directed to the tube wall [23]. Such an alternating direction of the velocity u in the central bundle cell, with the direction of the swirling velocity u_t over a large side of the oval tube profile remaining unchanged, is indicative of a spatial motion of the heat-transfer fluid, which enhances transfer processes. A vortex flow is observable in this case both in the spiral and the straight-through channels of a bundle. The directed convective flow of the heat-transfer fluid in the bundle cross section and the high level of turbulence generated by the wall and swirling jets with opposite rotation directions lead to an expansion of the flow core region and the formation of a thin boundary layer. It is characteristic of the boundary layer on twisted tubes that all components of the resultant velocity vector vary across the thickness from zero on the wall to a maximum on the outer edge at the flow core. The velocity in the flow core is practically unchangeable. Variations in the axial velocity u and in the resultant velocity vector V in the flow core are described by the universal logarithmic law, or the law of power $1/7$ [23]. The boundary layer thickness δ is defined by the empirical relation

$$\delta = A d_e \text{Fr}_M^{0.32} \quad (1.1)$$

where $A = 0.0349$ for δ_{\max} spiral channel, and $A = 0.0156$ for δ_{\min} in a straight-through channel [23]. The velocity u_t in the outer part of the boundary layer on twisted tubes (Fig. 1.5) varies by the law of a solid ($u_t r^{-1} = \text{const}$), i.e. the twisted tubes act as vortex filaments. All velocity components on the tube wall are equal to zero (Fig. 1.5). As demonstrated in ref. [3], maximum values of the velocities u_t and u_r in the bundle cross section account for about 10–20% of the axial velocity only on the outer edge of the boundary layer. In the flow core, the velocities u_t and u_r on the average make up a much smaller fraction of the axial velocity.

The flow in peripheral bundle cells differs somewhat in character from the flow in the central cells. As shown in ref. [3], the velocity u_t in the flow core of

peripheral cells is distributed by the law of circulation constancy ($u_\tau r = \text{const}$). Here, the direction of the velocity u_τ along the heat exchanger shell coincides with the twisting direction of the tube profile (Fig. 1.6). Thus, a vortex flow about the bundle axis forms in the peripheral region of a bundle, which contributes to some extent to heat and mass transfer with an azimuthal heat supply nonuniformity. From Fig. 1.6, which presents velocity components in orthogonal coordinates, it is evident that the exchange of fluid portions between the boundary layer and the flow core in the peripheral and central cells is similar in character, since the directions of the velocities u_r from the wall (+) and to the wall (-) are similar. In the flow core, a certain anisotropy of properties is observable which tends to a more isotropic structure at large Re numbers.

A very interesting structure of the shell-and-tube heat exchanger with twisted oval-profile tubes, whose straight circular ends are fixed in tube boards and which are relatively positioned to contact where an oval size is maximum is a device with tubes consisting of sections of length $(5 \dots 7) \cdot d$ with opposite twisting directions

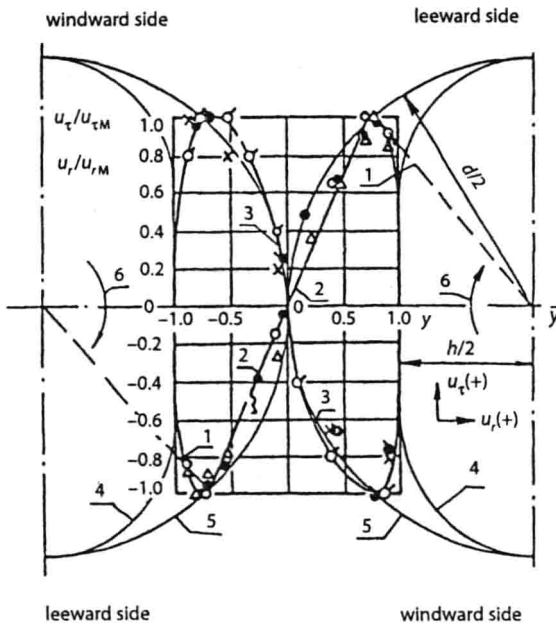


Fig. 1.5 Profiles of the tangential (u_τ) and radial (u_r) velocity components in central cells of a bundle with $Fr_M = 296$ [3]: \bullet , Δ , and \circ – experimental data for $u_\tau/u_{\tau M}$ at $Re = 10^4$, $1.5 \cdot 10^4$, and $6.7 \cdot 10^4$, respectively; \bullet , \star , and σ – the same for u_r/u_{rM} ; 1 – relation $u_\tau r^{-1} = \text{const}$; 2 – distribution of the velocity u_τ , generated by oppositely directed vortex filaments; 3 – profile of the radial velocity u_r ; 4 – oval profile of a twisted tube; 5 – conventional boundaries of spiral channels; and 6 – twisting direction of tubes.